

An Electrochemical Sensor for Determination of Sulfite (SO_3^{2-}) in Water Based on Molybdenum Disulfide Flakes/Nafion Modified Electrode

Jie Yang^{1,*}, Xiangyu Xu¹, Xuyan Mao¹, Liang Jiang¹, Xueliang Wang^{2,*}

¹ Bio-nanotechnology & Medical Engineering Institute, Jining Medical University, 272067, P. R. China

² School of chemistry and Chemical Engineering, Heze University, 27500, P. R. China

*E-mail: yangjiequst@126.com; qust-1977wxl@163.com

Received: 19 June 2020 / Accepted: 6 August 2020 / Published: 31 August 2020

The assay for monitoring the content of sulfite ions (SO_3^{2-}) is essentially important because sulfite has some seriously toxic effects on both environment and human health. For this, a SO_3^{2-} electrochemical sensor was fabricated utilizing molybdenum disulfide (MoS_2) and Nafion. The cyclic voltammetry (CV) and differential pulse voltammetry (DPV) showed that MoS_2 had excellently catalytical activity for the redox of SO_3^{2-} . After the conditions, such as the acidity of supporting electrolyte, scan rates, and other factors, for the electrochemical response of SO_3^{2-} were optimized, the proposed sensor showed a wide dynamic linear range from 5.0×10^{-3} to 0.5 mM ($r = 0.997$, $n = 15$) for determination of SO_3^{2-} with the limit of detection (LOD) of 3.3×10^{-3} mM, which can be applied for detecting the content of SO_3^{2-} in water with the advantages of good reproducibility, anti-interference, long-term stability and satisfactory recovery.

Keywords: MoS_2 ; Nafion; Sulfite; Nafion; Electrochemistry; Sensor

1. INTRODUCTION

Sulfite ions (SO_3^{2-}) is usually used as a perfect preservative in food industry for food and beverages storage because it has perfect effects for preventing oxidation, preserving vitamin C, inhibiting bacterial growth and controlling enzymatic browning reactions[1]. However, the SO_3^{2-} has some seriously toxic effects on both environment and human health. Sulfite ions (SO_3^{2-}) is the main existent formation in sulphur dioxide (SO_2) aqueous solution. In natural water, SO_3^{2-} can cause a detrimental effect on aquatic creatures by influencing the acid-base balance and depleting the dissolved oxygen [2]. For human being, it can cause asthmatic, allergic, mutagenic, and cocarcinogenic effects [3-6]. Thus, many organizations and countries, such as The World Health Organization (WHO) [7],

European Union (EU) [8], the United States Food and Drug Administration (FDA) [9], Brazil [10], and China[11], etc, have set up strict legislations to control and limit the maximum content of SO_3^{2-} in food or beverage. Therefore, the assay for monitoring the content of SO_3^{2-} is essentially important in human health and environmental safety. In present, fluorescence spectroscopy[12], high-performance liquid chromatography (HPLC) in combination with ultraviolet spectrophotometry[13], and chemiluminescence spectroscopy[14], were commonly used methods for routine detection of SO_3^{2-} , however, these methods are usually subject to time-consuming, sample pre-treatment and reagent preparation, and relative low sensitivity or precision. In recent years, the electrochemical sensors for determination of SO_3^{2-} based on chemically modified electrodes have attracted increasing attention due to the greater selectivity, sensitivity, reliability, and more possibility of on-line applications than traditional methods [2,15] .

Because direct electrochemical oxidation of SO_3^{2-} at conventional electrode involves high over potential [16,17], the amperometric sulfite-biosensors based on enzymes or nanostructured materials have been developed. The enzyme-based biosensors exhibit good sensitivity, accuracy, especially high selectivity due to the specificity of sulfite oxidase for catalyzing sulfite reaction [18-22], however, they were suffering from long-term stability due to the instability of enzymes. The nonenzymic sulfite-biosensors based on nanostructured materials have a lot of much better merits in stability, reproducibility and sensitivity relative to the enzyme-based biosensors because of the physico-chemical properties of nanostructured materials, such as large surface-to-volume ratio, distinctive electronic properties, stability and biocompatibility.

Molybdenum disulfide (MoS_2), the group VI family of transition metal dichalcogenides, exhibits a layered structure with each layer consisting of a molybdenum monolayer sandwiched by two sulfur layers, i.e., stacked S-Mo-S sheets in which Mo-S is bonded by a covalent bond and the S layers are connected by van der Waals forces [23]. The layered molybdenum disulfide, as another important family number of two-dimensional (2D) nanomaterials besides of graphene, has been extensively studied in various research regions, such as catalysts[24], rechargeable batteries[25], solar cells[26], solid lubricants[27] and sensors[28,29] owing to its chemical versatility and exceptional physicochemical properties, such as excellent mechanical properties, large specific surface areas, remarkable electronic performances, good chemical stabilities, high catalytic activities and facile synthesis processes[30].

In the reference of [28], our group studied the electrochemical behavior of SO_2 in two kinds of ionic liquids (ILs) ([EMIM][TfO] and [EMIM][BF₄]) using a MoS_2 /Nafion/glassy carbon electrode (MoS_2 /NF/GCE) and fabricated a sensor used to detect the content of SO_2 in fog and haze. Inspired by the reference of [28], in this research, we studied the electrochemicater behavior of SO_3^{2-} in water and set up an electrochemical method determination of SO_3^{2-} in water with wide dynamic linear range and low detection limit. This sensor exhibited good reproducibility, high selectivity, long-term stability and satisfactory recovery rate.

2. EXPERIMENTAL

2.1. Materials and instruments

All chemical reagents were of analytical or higher grade. α -Aluminum oxide polishing powder (purity $\geq 99.0\%$) was purchased from Alfa Aesar and the median diameter was 1.5 μm , 0.5-0.7 μm and 30 nm. Nafion solution (5 wt % alcohol solution) was purchased from Fluka Chemika. Sulphite ions (purity $\geq 98.0\%$) was supplied by Alfa Aesar. Potassium ferricyanide (purity $\geq 99.5\%$) and potassium ferrocyanide (purity $\geq 99.5\%$) were both purchased from Sigma-Aldrich. *N*-Methyl-2-pyrrolidone (NMP) and molybdenum disulfide (MoS_2) were obtained from Tianjin Kemiou Chemical Reagent Co. Ltd. (Tianjin, China). Deionized water was purified by a Milli-Q reagent water treatment system (Millipore, Milford, MA).

UV-vis spectra were acquired using a UV-2501PC spectrometer (Shimadzu, Japan). The wavelength was scanned from 700 to 400 nm in 1 nm steps. Scanning electron microscope (SEM) characterization was performed on an Ultraplus instrument (Zeiss, Germany) at 5.0 kV. The cyclic voltammetry (CV) and differential pulse voltammetry (DPV) experiments were performed on a CHI-660 D electrochemical workstation (CH Instruments, Shanghai, China) with a three-electrode system: a saturated calomel electrode reference electrode, a bare or modified glass carbon working electrode, and a Pt-wire counter electrode.

2.2 Preparation of layered MoS_2 suspension

The MoS_2 -NMP suspension of highly monodisperse monolayer MoS_2 sheets was prepared from commercial powder through lithium intercalation and exfoliation followed by extensive purification [31,32].

2.3 Fabrication of the modified electrodes

Prior to use, the glass carbon electrodes were pretreated by first polishing with 1.5 μm , 0.5-0.7 μm and 30 nm alumina powder. The electrodes were rinsed with deionized water and ultrasonically cleaned with ethanol and deionized water for 1 min to remove any remaining alumina, and then rinsed again with abundant deionized water. Successively, the electrode was pretreated by cycling the potential from 0.6 V to -0.2 V vs. the saturated calomel reference electrode (SCE) in 10 mM potassium ferricyanide-potassium ferrocyanide solution until reproducible voltammograms were obtained. Afterward, the electrode was rinsed with deionized water, left to dry at room temperature, and used without further modifications.

Three microliters of 0.2% Nafion solution diluted in ethanol was casted on the surface of the GC electrode, and it was allowed to dry at room temperature. This electrode was named the Nafion/GC electrode (NF/GCE). 3.0 μL of MoS_2 -NMP solution was coated onto the surface of the GC electrode and allowed to dry at room temperature. Then, another 3.0 μL Nafion-ethanol (0.2 % w/w) solution was

covered on the above-modified electrode and left to dry at room temperature. The electrode obtained by this process was named MoS₂/NF/GCE.

2.4 Electrochemical measurements

All the electrochemical measurements were carried out using a CHI 660 D model electrochemical workstation. In this study, the bare GCE, NF/GCE and MoS₂/NF/GCE electrodes were separately used as the working electrode to detect the electrochemical behavior of Na₂SO₃ prepared in a HAC-NaAC buffer solution. The electrochemical range was + 0.9 V to - 1.4 V and the scan rate was 50 mV/s.

The differential pulse voltammetry (DPV) was conducted with a pulse amplitude of 10 mV, a pulse width of 100 ms and a pulse period of 300 ms in the range of -1.25-0 V

3. RESULTS AND DISCUSSION

3.1 The characterization of MoS₂

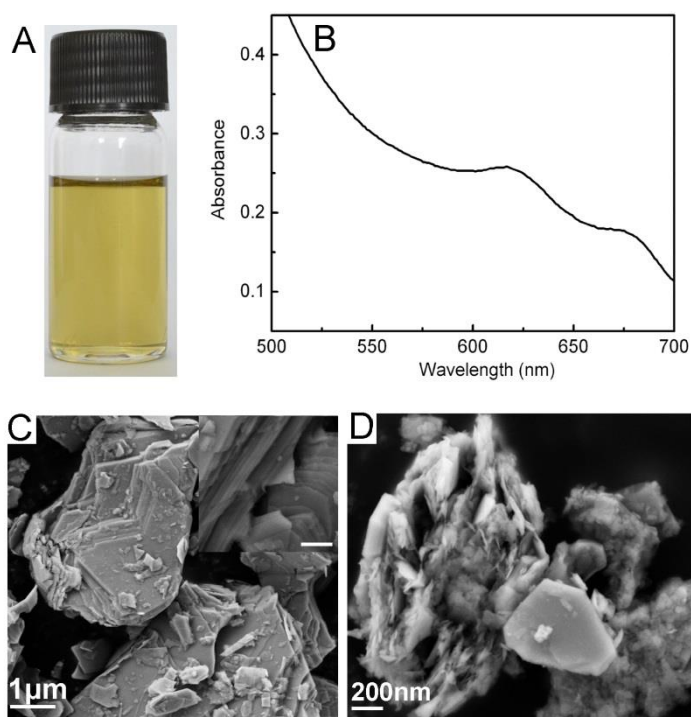


Figure 1. Optical image (A) and UV-vis spectrum of exfoliated MoS₂ (B). SEM image of MoS₂ powder (C) and exfoliated MoS₂ flakes (D).

The optical and structural characterization of the exfoliated MoS₂ flakes is shown in Figure 1. Figure 1A shows a typical chemically exfoliated MoS₂ dispersion in NMP. A representative absorption spectrum of MoS₂ dispersion was obtained by UV-vis spectrophotometry (Figure 1B). There were two

peaks centered at approximately 620 nm and 680 nm, characteristic of the 2H-MoS₂ phase [31]. These data suggested that the structure of the MoS₂ sheets was left mostly intact during the exfoliation process. Figures 1C and D illustrate SEM micrographs of commercial MoS₂ powder and the exfoliated MoS₂ flakes, respectively. As seen, the layer of exfoliated MoS₂ flakes was smaller than that in the commercial powder, and the exfoliated MoS₂ product formed by dense stacking of MoS₂ nanosheets.

3.2 Electrochemical response of SO₃²⁻ on different electrodes

The electrochemical response of 25 mM Na₂SO₃ on the three electrodes (GCE, NF/GCE and MoS₂/NF/GCE) was investigated (Figure 2). As seen in this figure, the oxidation potential (E_{pa}) and reduction potential (E_{pc}) on the MoS₂/NF/GCE were obtained at 0.120 V and -0.764 V, respectively (vs. SCE), and the peak-to-peak potential separation (ΔE_p) was 884 mV. On the NF/GCE, the E_{pa} and E_{pc} were, however, 0.132 V and -0.756 V, respectively, and the ΔE_p was expanded to 888 mV. On the bare GCE, ΔE_p were expanded further to 893 mV (the E_{pa} and E_{pc} were 0.110 V, -0.783 V, respectively). This result revealed that the reversibility of Na₂SO₃ on the MoS₂/NF/GCE was better than that on the other two electrodes. This may be attributed to the large specific surface area of the MoS₂ [33,34]. Meanwhile it has high catalytic activity, which can accelerate the electron transfer between the electrode surface and the measured substance. The exceptional physicochemical properties of the MoS₂ result in obviously increasing redox peak current of sulfite ions. The current is associated with the oxidation of SO₃²⁻ to SO₄²⁻ [35]. The results above prove that the MoS₂/NF/GCE can be used as a good sensor for SO₃²⁻.

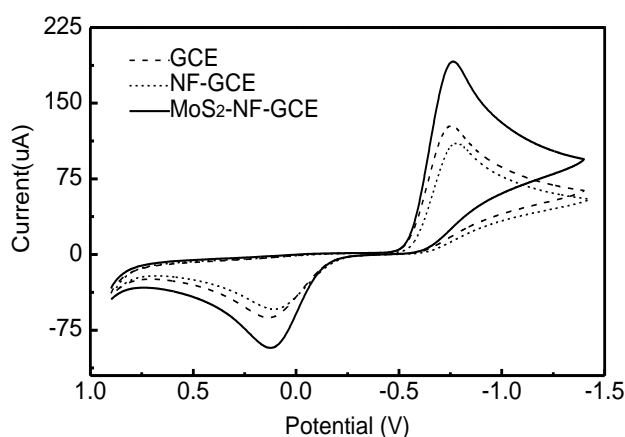


Figure 2. Cyclic voltammograms for the 25 mM Na₂SO₃ solution obtained on MoS₂/NF/GCE (*thick solid line*), bare GCE (*straight dash line*), and NF/GCE (*short dash line*). Scan rate 50 mV/s.

3.3 Differential pulse voltammetry of SO₃²⁻ on MoS₂/NF/GCE

The differential pulse voltammetry (DPV) of SO₃²⁻ on MoS₂/NF/GCE was obtained in different concentration of Na₂SO₃ solution. The results showed that the reduction peak current of SO₃²⁻ increased with its concentration (Fig. 3 A) and there was a good linear relationship between the peak

current and the concentration in the concentration range of 5.0×10^{-3} to 0.5 mM (Fig. 3 B). The linear equation is $y = 3.605 + 6.784 x$, with a correlation coefficient of 0.997 ($n = 15$, x is the value of Na_2SO_3 solution concentration, mM; y is the value of DPV peak current, μA). The limit of detection (LOD) was 3.3×10^{-3} mM, which was calculated as a signal equal to three times the standard deviation of the blank signal.

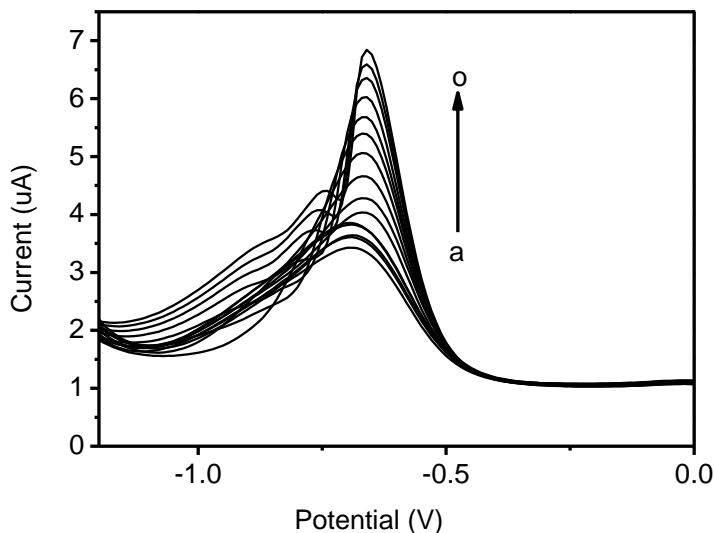


Figure 3 A. Differential pulse voltammetry curves on the $\text{MoS}_2/\text{NF}/\text{GCE}$ in different concentration of Na_2SO_3 solution (a-o: 5.0×10^{-3} , 1.0×10^{-2} , 1.5×10^{-2} , 2.0×10^{-2} , 2.5×10^{-2} , 5.0×10^{-2} , 0.1, 0.15, 0.2, 0.25, 0.3, 0.35, 0.4, 0.45, and 0.5 mM).

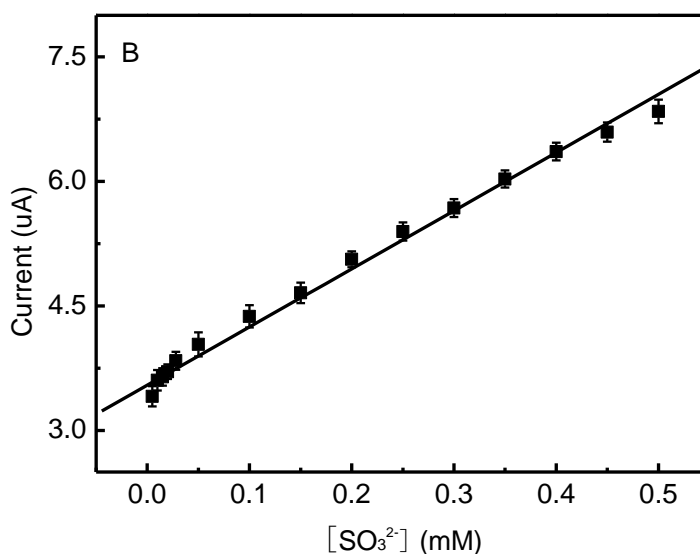


Figure 3 B. Plot of peak current vs. the Na_2SO_3 concentration.

The comparison of the proposed electrode with other modified electrodes for sulfite determination was list in Table 1. Although our sensor is somewhat inferior in sensitivity and detection limit, our sensor devices is cheaper, simple and easier to obtain than other sensors. At the same time, the electrode manufacturing method is more convenient.

Table 1. Comparison of different modified electrodes for sulfite determination.

Electrode	Detection Method	Linear range (mM)	Detection limit (mM)	Reference
Multi-walled carbon nanotubes /GCE	DPV	0.5-1.2	2.15×10^{-4}	[10]
Copper oxide nanosheet/GCE	DPV	0.3 -1.6	21.10	[15]
MoS ₂ -NF/GCE	DPV	5.0×10^{-3} - 0.5	3.3×10^{-3}	This work

3.4 Effect of pH values

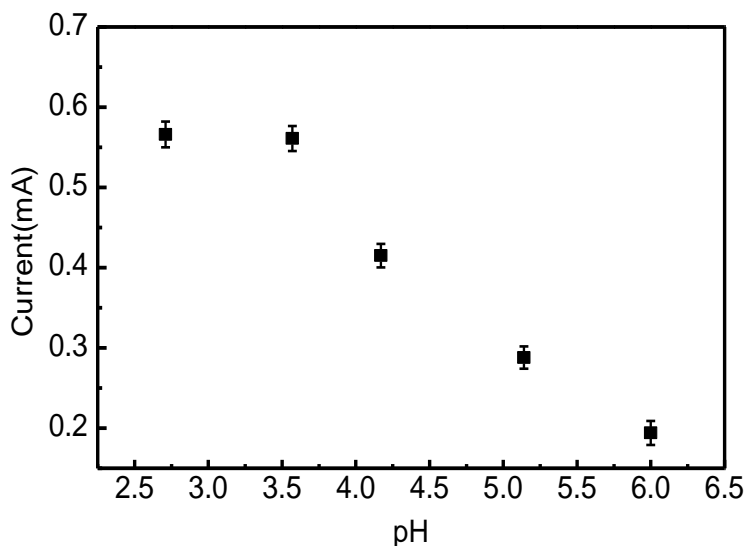


Figure 4. Correlation of peak currents obtained on MoS₂/NF/GCE with pH values.

The concentration of Na₂SO₃ in HAC-NaAC buffer solution with different pH values was fixed at 100 mM. The scan rate was 50 mV/s, and the potential range was + 0.9 V to -1.4 V. The cyclic voltammetric measurements were carried out using MoS₂/NF/GCE. The effect of a change in pH of the HAC-NaAC buffer on the peak current and peak potential in the pH range of 2.71 to 6.00 was observed. The peak current of the modified electrode decreased and the reduction in peaks was found to shift negatively as the pH values increased. The corresponding trend curve is shown in Figure 4, and

the results indicated that the peak current response was better with low background and good peak morphology at pH 3.58. Therefore, the cyclic voltammogram analyses were studied at pH 3.58.

3.5 Effect of scan rate

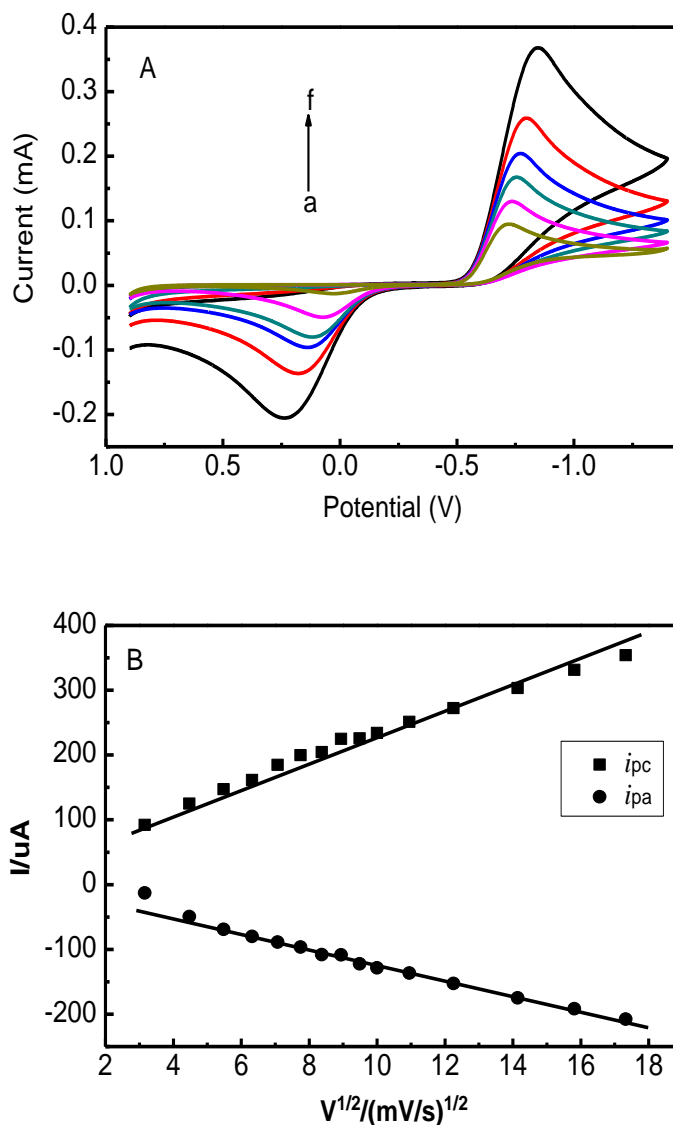


Figure 5. (A) Cyclic voltammograms obtained at different scan rates with MoS₂/NF/GCE; a-f: the scan rate was 10, 50, 100, 150, 250 and 300 mV/s. (B) A plot of peak current (I_p) vs. $v^{1/2}$ obtained with MoS₂/NF/GCE.

The relationship of peak currents and scan rates within the potential range of 10 mV/s to 300 mV/s was studied. Figure 7A presents the CVs of 25 mM Na₂SO₃ with MoS₂/NF/GCE at varying scan rates in HAC-NaAC buffer solution (pH = 3.58). The variations in scan rate affected the Na₂SO₃ response. It was found that with an increase in scan rate, the I_{pa} increased with a slight shift, and the E_{pa} moved toward the positive direction. Meanwhile, the I_{pc} also increased with increasing scan rate,

but the E_{pc} shifted in a negative direction. The best signal-to-background current characteristic was obtained with a scan rate of 50 mV/s.

Figure 5B shows the plot of the peak currents (I_p) vs. the square root of scan rate ($v^{1/2}$), which is a linear relationship. The linear equations were as follows: $I_{pa} = 5.7683 - 12.8181 v^{1/2}$ with a correlation coefficient (r) of 0.9901; $I_{pc} = 50.3964 + 18.0593 v^{1/2}$ ($r = 0.9952$). The plot of I_p vs. $v^{1/2}$ revealed that the electrochemical oxidation reaction of Na_2SO_3 on $\text{MoS}_2/\text{NF}/\text{GCE}$ is not controlled by the reaction between the $\text{MoS}_2/\text{NF}/\text{GCE}$ and the SO_3^{2-} in solution but controlled by diffusion.

3.7 Sample analysis

The content of SO_3^{2-} in tap water was determined using the $\text{MoS}_2/\text{NF}/\text{GCE}$ by DPV. The recovery test results are listed in table 2, suggesting a potential use of $\text{MoS}_2/\text{NF}/\text{GCE}$ as a sensor for sulfite anion.

Table 2 Recovery tests of real samples

Samples	Spiked (mM)	Total found (mM)	Recovery (%)
Tap water	0	0	-
	0.25	0.26	104.0
	0.11	0.11	100.0

Food samples such as red wines and ciders were also examined using the $\text{MoS}_2/\text{NF}/\text{GCE}$. The current intensity of SO_3^{2-} in red wine and cider obtained by DPV was 4.14 μA and 3.80 μA , respectively. Putting these data into the linear equation $y = 3.545 + 0.007x$ (as shown in Figure 3 B) for calculation of the amount of SO_3^{2-} in red wine and cider to be 5.44 mg/L and 2.33 mg/L, respectively. The results are in good accordance with the reference studies, suggesting a potential use of $\text{MoS}_2/\text{NF}/\text{GCE}$ as a sensor for sulfite anion.

4. CONCLUSIONS

A novel method for sulfite ions quantitation was examined with CV and DPV on a $\text{MoS}_2/\text{NF}/\text{GCE}$. The experimental conditions were optimized and chosen as pH value of 3.58 and scan rate of 50 mV/s. Meanwhile, the linear relationship between I_p and $v^{1/2}$ disclosed that the electrochemical oxidation reaction of Na_2SO_3 on this modified electrode is diffusion controlled. Under these optimum conditions, the proposed sensor showed great analytical property, including good linearity, low detection limit and high sensitivity, for determination of SO_3^{2-} in water.

ACKNOWLEDGEMENTS

This work was supported by the Natural Science Foundation of Shandong Province (ZR2017MB062 and ZR2017BB015), the Medicine and Health Project of Shandong Province (No. 2017WSB33045), Youth Scientific Research Foundation of Jining Medical University (No. JY2017KJ041) and Open Foundation of The Key Laboratory of Sensor Analysis of Tumor Marker, Ministry of Education, Qingdao University of Science and Technology (No. SATM201704)

References

1. D. Pearson, *Chem. Anal. Foods*, (1976) 40.
2. R. L. D. Tony, F. S. Marcos, *Electrochim. Acta*, 54 (2009) 4552.
3. J. G. Muller, R. P. Hickerson, R. J. Perez, C. Burrows, *J. Am. Chem. Soc.*, 119 (1997) 1501.
4. Z. Meng, N. Sang, B. Zhang, *Bull. Environ. Contam. Toxicol.*, 69 (2002) 257.
5. S. Satiaperakul, P. Phongdong, S. Liawruangrath, *Food Chem.*, 212 (2010) 893
6. U. T. Yilmaz, G. Somer, *Anal. Chim. Acta*, 603 (2012) 30.
7. WHO (2007) Expert committee of food additives sulfur dioxide. Cited accessed 07 Nov 2012.
8. European Commission Regulation 1493/1999, *Off J Eur Communities L* 179 1 2002
9. Anon. Sulfiting agents, *Fed. Reg.*, 51(1986) 25021.
10. V. Sudha, S. M. S. Kumar, R. Thangamuthu, *J. Alloys and Comounds*, 749 (2018) 990.
11. National Standard for Food Safety Food Additive Standard, National Standard of the People's Republic of China (GB 2760) (2011) Ministry of Health of the People 's Republic of China
12. C. Wang, S. Feng, L. Wu, S. Yan, C. Zhong, P. Guo, R. Huang, X. Weng, X. Zhou, *Sens. Actuators, B* 190 (2014) 792.
13. R. F. Mcfeeters, A. O. Barish, *J. Agric. Food Chem.*, 51 (2003) 1513.
14. X. Zhang, S. He, Z. Chen, Y. Huang, *J. Agric. Food Chem.*, 61 (2013) 840.
15. V. Sudha, K. Krishnamoorthy, S. M. S. Kuma, R. Thangamuthu, *J. Alloys and Compounds*, 764 (2018) 959.
16. Y. Zhang, L. Luo, Y. Ding, L. Li *Microchim. Acta*, 167 (2009) 123.
17. A. Isaac, J. Davis, C. Livingstone, A. J. Wain, R. G. Compton, *TrAC-Trends Anal. Chem.*, 25(2006) 589
18. Sroysee W., Ponlakheth K., Chairam S., Jarujamrus P., M. Amatatongchai, *Talanta*, 156 (2016) 154.
19. R. Spricigo, R. Dronov, F. Lisdar, S. Leimkuhler, F. W. Scheller, U. Wollenberger, *Anal. Bioanal. Chem.*, 393 (2009) 225.
20. A. K. Abass, J. P. Hart, D. Cowell, *Sens. Actuators B*, 62 (2000) 148.
21. A. B. Molinero, M. A. Alonso-Lomillo, O. Dominguez-Renedo, M. J. *Anal. Chim. Acta*, 812 (2014) 41.
22. J. Svitel, M. Stredansky, M. Pizzariello, A. Miertus, *Electroanalysis*, 10 (1998) 591.
23. P. C. Zhao, M. J. Ni, Y. T. Xu, C. X. Wang, C. Chen, X. R. Zhang, C. Y. Li, Y. X. Xie, J. J. Fei, *Sens. Actuators B*, 299 (2019) 126997.
24. L. Tang, X. G. Meng, D. H. Deng, X. H. Bao, *Adv. Mater.*, (2019) 1901996.
25. J. Xu, J. J. Zhang, W. J. Zhang, C. S. Lee, *Adv. Energy Mater.*, 7 (2017) 1700571.
26. S. Vijaya, G. Landi, J. J. Wu, S. Anandan, *Electrochim. Acta*, 294(2019)134.
27. J. Zhao, Y. Y. He, Y. F. Wang, W. Wang, L. Yan, J. B. Luo *Tribol. Int.*, 97 (2016) 14.
28. X. Xu, Z. Du, Y. Wang, X. Mao, L. Jiang, J. Yang, S. Hou, *J. Electroanal. Chem.*, 815 (2018) 220.
29. A. Aziz, M. Asif, G. Ashraf, M. Azeem, I. Majeed, M. Ajmal, J. L. Wang, H. F. Liu *Microchim. Acta*, 186 (2019) 671.
30. H. W. Hu, A. Zavabeti, H. Y. Quan, W. Q. Zhu, H. Y. Wei, D. C. Chen, J. Z. Ou, *Biosens. Bioelectron.*, 142 (2019) 111573.
31. P. Joensen, R. F. Frindt, S. R. Morrison, *Mater. Res. Bull.*, 21 (1986) 457.

32. G. Eda, H. Yamaguchi, D. Voiry, T. Fujita, M. W. Chen, M. Chhowalla, *Nano Lett.*, 11 (2011)5111.
33. J. G. Muller, R. P. Hickerson, R. J. Perez, C. J. Burrows, *J. Am. Chem. Soc.*, 119 (1997) 1501.
34. Z. Meng, N. Sang, B. Zhang, *Bull. Environ. Contam. Toxicol.*, 69 (2002)257.
35. N. Rea, B. Loock, D. Lexa, *Inorg. Chim. Acta*, 312 (2001)53.

© 2020 The Authors. Published by ESG (www.electrochemsci.org). This article is an open access article distributed under the terms and conditions of the Creative Commons Attribution license (<http://creativecommons.org/licenses/by/4.0/>).